HHS Public Access

Author manuscript

Neuroimage. Author manuscript; available in PMC 2020 August 15.

Published in final edited form as:

Neuroimage. 2019 August 15; 197: 761–771. doi:10.1016/j.neuroimage.2017.07.040.

Laminar fMRI: What can the time domain tell us?

Natalia Petridou[a,*] and **Jeroen C.W. Siero**[a,b]

[a]Radiology, University Medical Centre Utrecht, Utrecht, Netherlands [b]Spinoza Centre for Neuroimaging, Amsterdam, Netherlands

Abstract

The rapid developments in functional MRI (fMRI) acquisition methods and hardware technologies in recent years, particularly at high field (≥ 7T), have enabled unparalleled visualization of functional detail at a laminar or columnar level, bringing fMRI close to the intrinsic resolution of brain function. These advances highlight the potential of high resolution fMRI to be a valuable tool to study the fundamental processing performed in cortical micro-circuits, and their interactions such as feedforward and feedback processes. Notably, because fMRI measures neuronal activity via hemodynamics, the ultimate resolution it affords depends on the spatial specificity of hemodynamics to neuronal activity at a detailed spatial scale, and by the evolution of this specificity over time. Several laminar (≤1mm spatial resolution) fMRI studies have examined spatial characteristics of the measured hemodynamic signals across cortical depth, in light of understanding or improving the spatial specificity of laminar fMRI. Few studies have examined temporal features of the hemodynamic response across cortical depth. Temporal features of the hemodynamic response offer an additional means to improve the specificity of fMRI, and could help target neuronal processes and neurovascular coupling relationships across laminae, for example by differences in the onset times of the response across cortical depth. In this review, we discuss factors that affect the timing of neuronal and hemodynamic responses across laminae, touching on the neuronal laminar organization, and focusing on the laminar vascular organization. We provide an overview of hemodynamics across the cortical vascular tree based on optical imaging studies, and review temporal aspects of hemodynamics that have been examined across cortical depth in high spatiotemporal resolution fMRI studies. Last, we discuss the limits and potential of high spatiotemporal resolution fMRI to study laminar neurovascular coupling and neuronal processes.

Keywords

Ultra-high field; 7T; laminar fMRI; spatiotemporal characteristics; hemodynamic response; onset

*Corresponding author (N.Petridou@umcutrecht.nl).

Introduction

Over the past two decades, functional MRI (fMRI) has offered unprecedented advances in our understanding of human brain function. Particularly in recent years, rapid developments in accelerated parallel imaging (Barth et al., 2016, Feinberg and Yacoub, 2012) and MRI hardware technologies (such a signal reception coils, Petridou et al., 2013; Wiggins et al., 2009; Wiggins et al., 2006) and high performance gradients (Ugurbil et al., 2013) have dramatically boosted our capability for detailed and fast imaging of the brain. High field (≥ 7T) fMRI in particular has enabled unparalleled visualization of functional detail at a laminar or columnar level in confined parts of the brain (see Dumoulin et al., 2017 for review), bringing fMRI close to the intrinsic resolution of brain function. High resolution fMRI has thus the potential to be a valuable tool to study the fundamental processing performed in cortical micro-circuits, and their interactions such as feedforward and feedback processes.

This potential, however, does not come without challenges. One challenge is that the hemodynamic response that is typically measured evolves at a slower temporal scale than neuronal processes, on the order of seconds versus on the order of milliseconds. A second challenge is that the spatial specificity of the measured hemodynamic response must be very precise at a fine (<1mm) spatial scale, and ideally concomitant with the capillary bed that serves active neuronal sites (Harrison et al., 2002). Depending on the acquisition method used, the fMRI signal can consist of a mix of hemodynamic changes, some of which relating to neuronal activity via micro-vessels, and some of which relating to the organization of the different vessel sizes (micro-and macro-vessels) within the volume imaged (Kim and Ogawa, 2012). Thus, the ultimate resolution of fMRI depends on the concomitance of hemodynamics and neuronal activity at a detailed spatial scale, and by the evolution of this concomitance over time.

The majority of laminar (≤1mm spatial resolution) fMRI studies, in animals and humans, have focused on the characterization or the improvement of the spatial specificity of fMRI to the microvasculature (capillary bed), often examined in terms of spatial patterns or signal profiles across cortical depth (Ahveninen et al., 2016; De Martino et al., 2013; Fracasso et al., 2017; Goense et al., 2012; Goense and Logothetis, 2006; Goense et al., 2007; Guidi et al., 2016; Harel et al., 2006; Herman et al., 2013; Huber et al., 2014; Huber et al., 2015; Jin and Kim, 2008b; Kemper et al., 2015; Kim and Kim, 2010; Koopmans et al., 2010; Koopmans et al., 2011; Polimeni et al., 2010; Poplawsky et al., 2015; Ress et al., 2007; Scheeringa et al., 2016; Shih et al., 2013; Zhao et al., 2006; Zhao et al., 2004). Some studies, notably with the combination of sub-millimeter blood-oxygenation-level-dependent (BOLD) fMRI and computational data analysis approaches, have explored neuronal processes across laminae via hemodynamic inference, for example receptive field size (Fracasso et al., 2016), tuning (De Martino et al., 2015; Olman et al., 2012), or feedback processes (Kok et al., 2016).

Few fMRI studies to date have examined temporal features of the hemodynamic response across cortical depth (Gardumi et al., 2017; Hirano et al., 2011; Jin and Kim, 2008a; Shen et al., 2008; Siero et al., 2015; Siero et al., 2011; Siero et al., 2013; Silva and Koretsky, 2002;

Silva et al., 2007; Silva et al., 2000; Tian et al., 2010; Uludag and Blinder, 2017; Yu et al., 2012; Yu et al., 2016; Yu et al., 2014; Zhao et al., 2007). These studies used BOLD but some also cerebral blood volume weighted (CBV) or cerebral blood flow (CBF) weighted measurements, and observed similar spatiotemporal features in the hemodynamic response measured with fMRI to those measured with invasive optical imaging in animals. Optical imaging permits hemodynamic measurements at the level of individual vessels, albeit with limited sensitivity in deeper cortical layers, and has played a key role in our understanding of the mechanisms of hemodynamics (see Hillman, 2014 for review). Optical measurements point to a finely orchestrated hemodynamic response upon neuronal activation that is initiated in the capillary bed and that is followed by upstream (toward cortical surface) and downstream (toward local capillary beds and venous network) propagation (Chen et al., 2011; Chen et al., 2009; Iadecola et al., 1997; Tian et al., 2010). High spatiotemporal resolution 7T fMRI in humans revealed faster BOLD responses at middle or deeper cortical depth in the motor and visual cortex, where higher microvascular density was expected (Siero et al., 2011; Siero et al., 2013). In higher resolution animal studies, faster responses were associated with the microvasculature and with cortical layers where neuronal processing apparently initiated (Hirano et al., 2011; Silva and Koretsky, 2002; Yu et al., 2012; Yu et al., 2014).

These findings suggest that the temporal evolution of hemodynamics could offer an additional means to improve the specificity of fMRI to the microvasculature, particularly for gradient-echo-based BOLD fMRI that is sensitive to signals from all vessel sizes. Temporal features of the hemodynamic response could help target neuronal processes and neurovascular coupling relationships across laminae, for example by differences in the onset times of the response across cortical depth, and potentially inform on both the spatial location and temporal profile of the neuronal response across laminae.

In this review, we discuss factors that affect the timing of responses across laminae, touching on the neuronal laminar organization in the context of temporal dynamics, and focusing on the laminar vascular organization. We review hemodynamics across the cortical vascular tree based on optical imaging studies, and temporal aspects of hemodynamics that have been identified in laminar fMRI studies. Finally, we discuss the limits and potential of high spatiotemporal resolution laminar fMRI to elucidate neurovascular coupling, stages of neuronal activity, and neuronal processes across laminae.

What affects the timing of responses across laminae?

Neuronal organization

The cerebral cortex is organized into 6 layers (Brodmann, 1909) comprised of different cellular composition and connections. Histology studies in visual cortex have shown that the laminar distribution of afferent synapses can dissociate inputs from thalamo-cortical and cortico-cortical (e.g. higher to lower order areas) connections (Felleman and Van Essen, 1991). Layer 4 (internal granular layer) predominantly receives input via feed-forward, thalamo-cortical afferents (Hubel and Wiesel, 1972; Tigges et al., 1977), whereas feedback cortico-cortical and thalamo-cortical projections arrive mainly on superficial (supra-granular, layers 1–3) and deep (infra-granular, layers 5–6) layers, avoiding the location occupied by

thalamo-cortical afferents (Graham et al., 1979; Rockland and Pandya, 1979; Tigges et al., 1977). Lateral fibers on the other hand target all three main compartments indistinctively (infra-, granular, and supra-granular, Felleman and Van Essen, 1991)

Histology findings are also supported by electrophysiology studies. Laminar recordings in visual cortex have shown that input to layer 4 is associated with a rapid electrophysiological response in that layer, followed by a sequence of responses (current sinks) in supra- and infra-granular layers (Givre et al., 1994; Maier et al., 2011; Mitzdorf and Singer, 1979; Schroeder et al., 1998; Schroeder et al., 1991; Self et al., 2013). Self et al reported that input activity in layer 4 of primary visual cortex arises as early as 40ms after stimulus onset, followed by activity in supra- and infra- granular layers at about 60ms (Self et al., 2013). Schroeder et al (1998) examined the stages of activity across laminae in the dorsal and ventral streams of visual cortex; for visual areas in the dorsal stream, the authors also reported that the first synaptic activity was observed in layer 4 followed by activity in supra- and infra-granular layers, similar to primary visual cortex. For areas in the ventral stream, however, the first activity was distributed across laminae indicative of a neuronal modulation as opposed to feedforward excitation. The authors proposed a hierarchical cortical organization comprising of serial and parallel temporal components (Schroeder et al., 1998). In theory, a laminar profile of the initial stages of neuronal activity could reveal the direction of information flow and local neuronal processing.

In addition to the initial stages of neuronal activity, the temporal profile of ongoing neuronal activity can vary across laminae. For example, sustained responses in local field potentials (LFP), i.e. responses that are not time-locked to the stimulus onset, have been observed in infragranular layers in visual cortex, mainly in frequencies below 50Hz (Maier et al., 2011). Differences in the temporal profile of activity have also been reported between upper and deeper laminae, across a broad range of frequencies during visual stimulation and at rest (Maier et al., 2010). Low frequencies (< 30Hz, such as the alpha band at 8–12Hz) have been associated with deeper cortical layers, and higher frequencies (> 30Hz) have been associated with granular or upper cortical layers (Buffalo et al., 2011; Haegens et al., 2015; Maier et al., 2010; Maier et al., 2011; Spaak et al., 2012; Xing et al., 2012). Taken together, these findings suggest that the temporal profile of ongoing activity across laminae reflects differences in local neuronal processing.

Vascular architecture

The intra-cortical vascular system is also organized in layers according to vascular density (4 layers), or penetration depth and vessel diameter (5 groups) (Duvernoy et al., 1981; Reina-De La Torre et al., 1998). Within the cortex, vessels can be broadly classified as micro-vessels (capillary bed, diameters ~5μm) and macro-vessels (diameters ~>10μm) (Duvernoy et al., 1981).

Depending on penetration depth and diameter, intra-cortical macro-vessels can be further classified into 5 groups (Duvernoy et al., 1981): vessels in groups 1 and 2 penetrate supra-granular layers (vessel diameters 10–25μm and 20–30μm for arteries and veins respectively), vessels in group 3 penetrate middle cortical layers (layers 3–5, vessel diameters 15–30μm and ~45μm for arteries and veins respectively), vessels in group 4 penetrate deeper cortical

layers (layer 6, vessel diameters 30–40μm and ~65μm for arteries and veins respectively), and vessels in group 5 penetrate to white matter, with branches in gray matter as well (vessel diameters 30–74μm and 80–125μm for arteries and veins respectively) (Figure 1A, see Kim and Ogawa, 2012 for review). Pial vessels at the cortical surface are relatively larger (diameters ~> 100μm), and more sparse as compared to intra-cortical vessels (Duvernoy et al., 1981).

Depending on vascular density, intra-cortical micro-and macro-vessels can be categorized into 4 vascular layers (Figure 1B) (Duvernoy et al., 1981; Reina-De La Torre et al., 1998). Vascular density is higher in cortical layers with higher cellular density although vascular density variation across laminae is less distinct than cellular density variation (Adams et al., 2015; Blinder et al., 2013; Tsai et al., 2009). The highest vascular density is reported in middle cortical layers (Duvernoy et al., 1981), for example capillary density is higher in layer 4 in primary visual (Bell and Ball, 1985; Weber et al., 2008), and somatosensory (Blinder et al., 2013; Masamoto et al., 2004) cortices. A higher density of venules as compared to arterioles has been reported in supra-granular cortical layers, while middle and deep cortical layers contain a higher density of arterioles as compared to venules, indicating more venous-weighting toward the pial surface (Blinder et al., 2013).

Overall, the intracortical vascular architecture suggests a match between hemodynamics and expected cellular metabolic demand across laminae (Adams et al., 2015; Duvernoy et al., 1981).

Hemodynamics across the vascular tree; insights from optical imaging

Optical imaging is based on illumination of tissue with light at different wavelengths, which can be chosen to be sensitive to oxy-hemoglobin (HbO), deoxy-hemoglobin (HbR), and total hemoglobin changes (HbT). Recordings of reflected light can be obtained at very high spatial and temporal resolution, enabling visualization of rapid hemodynamic changes in individual vessels, also informing on blood volume and flow. The penetration depth within cortex varies depending on the method and/or wavelength used, ranging from the pial surface to few mm in cortex (Devor et al., 2012). Optical imaging studies, often with accompanying electrophysiological data, have played a key role in shaping our understanding of hemodynamics across the vascular tree and have provided critical insights on the mechanisms of the fMRI signal (Hillman, 2014). Here we discuss some of these studies to provide an overview of hemodynamics across the vascular tree, focusing on recent optical imaging methods that allow improved visualization across cortical depth.

The evolution of the hemodynamic response across the vascular tree can be summarized as initiating in the capillary bed and followed by upstream (arterial network towards the pial surface) and downstream (in local capillary beds and venous network) propagation (Chen et al., 2011; Chen et al., 2009; Iadecola et al., 1997; Srinivasan and Radhakrishnan, 2014; Tian et al., 2010), illustrated in Figure 2.

The spatial extent of the hemodynamic response changes over time, being more focal to neuronal activity at early stages of the response, and then spreading both across cortical

depth and laterally across the cortex (Chen et al., 2011; Chen et al., 2009; Devor et al., 2007; Iadecola et al., 1997; Srinivasan and Radhakrishnan, 2014; Tian et al., 2010).

Stimulation of the rat paw, and ensuing neuronal activation in somatosensory cortex, results in a rapid hemodynamic response that initiates in the capillary bed in middle (input) cortical layers, approximately 0.5 seconds after the stimulus onset (Chen et al., 2011; Tian et al., 2010), in line with earlier reports in cat visual cortex (Malonek and Grinvald, 1996, Malonek et al., 1997). This rapid hemodynamic response is observed as increases in HbT (Chen et al., 2011; Culver et al., 2005; Hillman et al., 2007; Sirotin et al., 2009) or red blood cell content (Srinivasan and Radhakrishnan, 2014), indicative of a rapid and local increase in blood volume (Stefanovic et al., 2008). This response has been associated with a local dilation of capillaries (Stefanovic et al., 2008; Tian et al., 2010), however, whether capillaries can dilate actively via local control of their diameter is controversial (Hall et al., 2014; Hill et al., 2015). This response has also been associated with the 'initial dip' sometimes observed in BOLD (Sirotin et al., 2009), although the initial dip may also be indicative of metabolic processes associated with changes in HbR (Grinvald et al., 2000; Malonek and Grinvald, 1996; Vanzetta et al., 2005). Changes in HbR have been reported to precede (Berwick et al., 2005, Vanzetta et al., 2005), roughly coincide (Malonek et al., 1997), and follow (Hillman et al., 2007; Sirotin et al., 2009, Berwick et al 2008) changes in HbT, and the spatial extent of HbR change has been reported to be both more confined (Dunn et al., 2005) and more diffuse (Sirotin et al., 2009) than that of HbO and HbT, although these discrepancies could be due to differences in experimental conditions between studies (e.g. different optical imaging methods, rodent vs awake macaque). Changes in HbO follow changes in HbT and HbR (Hillman et al., 2007; Sirotin et al., 2009, Malonek et al., 1997, Berwick et al., 2005, Berwick et al., 2008).

Upstream arterial dilation rapidly follows the initial hemodynamic response (Chen et al., 2011; Chen et al., 2009; Devor et al., 2007; Iadecola et al., 1997; Srinivasan and Radhakrishnan, 2014; Tian et al., 2010), and can be observed at about 200 ms after the initial response (Chen et al., 2011; Tian et al., 2010). For some pial arteries, dilation across the cortical surface can extend further than 1mm from the responding capillary beds (Chen et al., 2011), and the time to peak of the hemodynamic response can lag by about 1–2 seconds as compared to the vessels deeper in the cortex (Chen et al., 2009; Malonek et al., 1997), likely reflecting the speed of dilation propagation across the arterial vascular tree. Arterial dilation leads to increases in blood flow and decreases in blood transit times, the earliest of which is observed in the capillary bed (Merkle and Srinivasan, 2016; Stefanovic et al., 2008). Interestingly, changes in HbR have been reported in the arterial compartment (Hillman et al., 2007; Berwick et al., 2005) suggesting that oxygen saturation is not as high as expected (~98%), in agreement with oxygen tension measurements of branching or surface arterioles in rat cortex during forepaw stimulation (Vazquez et al., 2010), and further suggesting that arterioles may contribute to the BOLD signal (Hillman et al., 2007; Vazquez et al., 2010).

In the venous compartment, the earliest signal observed is a change in HbT at approximately the same time as arterial dilation (Hillman et al., 2007; Berwick et al., 2005). The change in HbT is followed by a delayed change in HbR and HbO, by about 500 ms, which can be

associated with the transit time of blood with increased oxygenation levels through the capillary bed (Hillman et al., 2007). Dilation in venules or the venous compartment likely does not occur for short stimulus durations (<4s), indicating that the observed HbT change reflects a change in blood flow (Hillman et al., 2007). However venous dilation has been observed for longer stimulus durations (about >10s), that persists after stimulus cessation, indicating a blood volume increase in the venous compartment (Drew et al., 2011). Prolonged stimulation can also lead to a reduction of the response in pial arteries and a 'plateau' in the hemodynamic response in the capillary bed (Berwick et al., 2008). The overall hemodynamic response lasts longer than neuronal activation.

The return to baseline is first observed in the periphery of the presumed stimulated cortical region, for both the capillaries and arterial compartment. In the capillary bed coinciding with the stimulated cortical region, HbT and red blood cell content, reflecting blood volume, remain elevated, and are the last to return to baseline (Berwick et al., 2008; Chen et al., 2011; Hillman et al., 2007; Srinivasan and Radhakrishnan, 2014). After return to baseline, a reduction in flow by vasoconstriction can be observed in the pial and branching arteries, i.e. in superficial layers of the cortex, that could be associated with the "post-stimulus undershoot" observed with fMRI (Chen et al., 2011; Hillman et al., 2007; Srinivasan and Radhakrishnan, 2014).

In sum, early stages of the hemodynamic response are rapid, on the order of 500ms, and co-localize with the capillary beds that serve active neuronal sites. Rapid changes can also be observed on the venous side as blood leaves the capillary bed, at about 200–500ms after the onset of the response, with flow changes preceding oxygenation changes by about 300ms. The spatial extent of the response spreads over time in macro-vessels. Upon return to baseline, increased blood volume (and venous outflow) persists in the capillary bed longer than in arterial macro-vessels.

In principle, the early phase of the hemodynamic response could allow for improved specificity to active neuronal sites, and potentially allow to disentangle neurovascular coupling and neuronal processing across laminae. In the context of fMRI, the earliest and most specific responses would be observed as changes in CBV, possibly the 'initial dip' if detectable, followed by the onset of BOLD and CBF.

Temporal features of hemodynamics detected with (laminar) fMRI

As event-related fMRI was introduced it enabled detailed time course analysis of fMRI activation allowing researchers to look beyond the static activation patterns at the dynamic aspects of fMRI activation (Buckner et al., 1996; Friston et al., 1998). The ultimate goal is to study the temporal sequence of neuronal events and the neuronal communication pathways in the human brain. The latter can be studied between brain regions as whole, but also among the different cortical laminae which we know contain differences in local neuronal innervation and processing in terms of input and output information flow as discussed earlier. Here we summarize and discuss the work on laminar fMRI time course analysis in animals and recent findings in human studies that capitalize on the increased sensitivity of ultra-high field MRI.

Animal studies

The work by Silva et al was first to resolve distinct temporal features of BOLD, CBF and later also CBV fMRI time courses across cortical depth in rat somatosensory cortex. (Silva and Koretsky, 2002; Silva et al., 2007; Silva et al., 2000). Capitalizing on fast sampling (108ms) and high in-plane spatial resolution (470μm), CBF and BOLD response onset times and time-to-peak (TTP) were obtained in deep and surface cortical regions. CBF responses preceded BOLD responses for both regions, approximately by 0.5s for deep cortical regions, likely caused by the arteriole-venule transit time (Silva et al., 2000). BOLD responses in deep regions were notably faster compared to surface regions. Using an even higher in-plane spatiotemporal resolution, 200μm and 40ms, Silva and Koretsky resolved detailed BOLD time courses, measuring response latencies in laminar regions 1–3, 4–5 and 6 (Silva and Koretsky, 2002) (Figure 3A). Shortest onset time and TTP were found in thalamo-cortical input layer 4 of 0.59s and 4.13s respectively for a 4s stimulation duration. It was proposed that laminar specific onset times of the BOLD response have the potential to enable the study of laminar neuronal communication and events. Although the vasculature is not as fast as neuronal events, the authors argue that the vasculature and laminar neurovascular coupling can be organized to follow the neuronal electrical activity as closely as possible. Later work by Silva et al compared BOLD and iron-oxide derived CBV responses across cortical layers using an efficient event-related design, an m-sequence, using very brief forelimb stimulation pulse durations of 0.33ms presented during a 0.5–1s period, allowing estimation of the BOLD and CBV impulse response function (Silva et al., 2007). Compared to the BOLD response, the full-width-at-half-maximum (FWHM) and TTP of the CBV response was markedly reduced, both by approximately 0.7s, and their spatial maps were more homogeneous. The faster CBV response indicates a dominating contribution from arteriole vessel dilations, as opposed to the venous dominated delayed BOLD response. The CBV response was found spatially more confined to the forelimb area, again as it is likely mostly devoid of macrovascular contributions. The authors also reported a slow prolonged CBV response purportedly as a result of two different contributing vascular compartments (arteriolar and/or capillary and/or venous). This would be in line with a prolonged HbT and red blood cell content observed with optical measurements (Berwick et al. 2008; Chen et al., 2011; Hillman et al., 2007; Srinivasan and Radhakrishnan, 2014), although the reported time window in these studies was shorter. It should be noted, however, that MRI measurements are obtained across the entire cortical depth, unlike most optical imaging measurements, albeit at different spatial/temporal resolutions, therefore caution should be exercised when directly comparing the two modalities. No post-stimulus undershoot was observed for either BOLD or CBV response.

A large body of work in animals, mostly in rats and cats, further explored the temporal features of the BOLD response across cortical depth. Most studies complement the cortical-depth resolved BOLD measurements with CBV and/or CBF measurements but some also with optical imaging measurements. This offers a multimodal view and thus a more in-depth characterization and understanding of the temporal features of the BOLD response across cortical depth. In addition to the positive BOLD response, also negative BOLD response components such as the post-stimulus undershoot and the initial dip have been a topic of interest. These topics are discussed separately below.

Temporal dynamics of the positive BOLD response across cortical depth such as onset time, TTP, FWHM, and including stimulation duration dependence have been intensively studied (Jin and Kim, 2008a; Shen et al., 2008; Hirano et al., 2011; Tian et al., 2010; Kim and Kim, 2011). A general finding is that the early phase of the BOLD response, and thus shortest onset times, are localized to the middle cortical regions. This is in line with an earlier proposed notion that the early phase of the BOLD response originates from the microvasculature (Lee et al., 1995; Menon and Goodyear, 1999), serving directly the gray matter parenchyma, which can be used to improve spatial localization.

Work by Jin et al in cat visual cortex examined BOLD, CBF, and MION-derived CBV responses across cortical depth during 60s stimulation (Jin and Kim, 2008a). The spatial specificity of the BOLD response showed a time dependent behavior where the very early phase of the response was confined to middle cortical regions. Onset times in middle cortical regions were estimated on the order of ~1.35s, whereas upper regions were more delayed with onset times of ~1.8s. Note the longer onset times compared to rat somatosensory cortex reported by Silva et al (Silva and Koretsky, 2002; Silva et al., 2007; Silva et al., 2000). The onset of the CBV response was on the order of 1s, faster than the BOLD response, and had longer TTP in middle cortical regions than upper cortical regions. This is in line with Silva et al in rat somatosensory cortex, however these authors found increased CBV TTP specifically for layer 6 (Silva et al., 2007). The CBV response showed the strongest specificity to middle cortical regions at later time points, whereas the CBF response was nearly time independent (Jin and Kim, 2008a). Interestingly, the relationship between CBV and CBF responses showed a spatial and temporal mismatch, indicating that care should be taken for high-resolution studies on dynamic quantification of CMRO2 changes across cortical depth when using conventional BOLD biophysical models such as the Davis' model.

It is suggested that the venous vasculature, probed by the BOLD contrast, takes longer time to dilate than feeding arterioles probed by MION-derived CBV fMRI, specifically for the relatively long stimulus durations as employed in Jin et al (Jin and Kim, 2008a). This is in line with a prolonged venous dilation for long stimuli observed with optical measurements (Drew et al., 2011) This is also in line with Kim et al who reported in cat visual cortex that increases in arterial CBV are dominant for short stimulus durations, while venous CBV contribution increases for long stimulus durations (Kim et al., 2007; Kim and Kim, 2011). For long stimulus durations, the amplitude of arterial CBV and total CBV showed higher specificity to middle layer 4 of cat visual cortex during visual stimulation, while the amplitude of venous CBV was not layer-specific. The high specificity to middle cortical layers of the CBV (total and/or arterial) response notably at later time points could be used to improve spatial localization of these layers. This notion was also recently shown in rat olfactory bulb by Poplawsky and colleagues; the later phase of the CBV response was highly specific to the associated neuronal active layers (Poplawsky et al., 2015). The spatial specificity of the CBV response to middle cortical layers at later time points would be in line with the observation of elevated HbT and red blood cell content in parenchymal regions in optical imaging studies (Berwich et al, 2008; Chen et al., 2011; Hillman et al., 2007; Srinivasan and Radhakrishnan, 2014

A study in rat somatosensory cortex by Tian et al, compared two-photon microscopy measurements of single blood vessel dilations (arterioles and capillaries) with BOLD fMRI responses at different cortical depths (Tian et al., 2010). The two-photon microscopy results show an upstream vasodilation along penetrating arterioles followed by downstream propagation towards local capillary beds. The positive BOLD responses lagged with respect to the vessel dilation responses by >0.5s across all measured cortical depths. Shortest BOLD response onset times (~1s) were found in the middle cortical layers, and the slowest responses (~1.5s) in layer 1. The onset times for middle cortical layers are longer compared to the findings by Silva et al (0.59s, Silva and Koretsky, 2002; Silva et al., 2007), which is likely due to a lower spatiotemporal resolution and different definition of onset time.

The effect of stimulus duration on the spatiotemporal characteristics of BOLD, iron-oxide derived CBV, and CBF responses across cortical layers was studied by Hirano et al in rat somatosensory cortex (Hirano et al., 2011). They showed that a single ultra-short stimulation pulse of 0.33ms can be robustly detected, eliciting distinct BOLD, CBV, CBF response across cortical layers that varies strongly with stimulus duration. BOLD responses showed longest onset times and TTP, and increased FWHM compared to the CBF and CBV responses. The shortest onset times (~0.5s) and TTP were found in upper and middle cortical layers. Onset times for CBV in layers I-3 and 4–5 where shorter than for BOLD but not different from CBF onset times. No onset time differences were found between upper and middle cortical layers, in contrast with earlier work by Silva et al (Silva 2002), which can be due to differences in field strength, contrast-to-noise ratio, and spatiotemporal resolution used. The onset time for BOLD was on the order of 0.1s longer than that of CBV/CBF, which is shorter than the transit time of blood from arterioles to venules (0.5s, and suggests that arterioles may contribute to the BOLD signal, as noted in the previous section (Vazquez et al., 2010). Longer stimulation (>=1s) prolongs the BOLD and CBV response, observed as prolonged offset tail for CBV as in Silva et al (Silva et al., 2007). The CBF response was not prolonged, indicating a passive venous contribution and dispersive behavior for the CBV response at these time points for longer stimulation. Short stimuli, as compared to the arterial-venous transit time, ensure a tight temporal relationship between CBV and CBF responses during dilation as well as vasoconstriction upon stimulus cessation. Longer stimulus duration causes passive accumulation of blood in the venous side, therefore very short stimulus durations are recommended to study laminar neurovascular coupling relationships (Hirano et al., 2011).

A BOLD post-stimulus undershoot is typically observed after stimulus cessation and reflects a transient increase in local deoxyhemoglobin (HbR) that can arise from multiple biophysical processes: i) delayed vascular compliance, i.e. elevated venous CBV, ii) remaining elevated cerebral metabolic rate of oxygen (CMRO2), iii) an undershoot in CBF, and combinations of the above (Chen and Pike, 2009; Hill et al., 2015; Shmuel et al., 2007; Yacoub et al., 2006). The post-stimulus undershoot origin and its spatial dependence, notably across cortical depth, is topic that has seen considerable attention but also debate. Negative BOLD components such as the post-stimulus undershoot may reflect more neuronal specific properties than positive BOLD components and potentially be more spatially locked to nearby neuronal activity. In addition, investigations of the post-stimulus

undershoot across cortical depth can shed light on the metabolic support and neurovascular coupling, but also uncoupling, of the BOLD response.

The intracortical spatial dependence of the post-stimulus undershoot was studied in detail by Zhao et al in cat visual cortex (40s stimulation) using BOLD and MION-derived CBV responses (Zhao et al., 2007). The post-stimulus undershoot of the BOLD response was found to peak in middle cortical layers, and coincided with the largest CBV changes during stimulation. The middle cortical layers also revealed a post-stimulus CBV increase albeit with much smaller amplitude and faster recovery to baseline than the BOLD post-stimulus response. The results by Zhao et al potentially support a metabolic origin for the BOLD post-stimulus undershoot as the dominant contributor, however alternative explanations such as the elevated post-stimulus CBV and possible CBF decreases cannot be ruled out and may in fact jointly contribute to the post-stimulus BOLD signal and possibly with different temporal behavior. Zhao et al also indicated that the post-stimulus undershoot can improve the spatial localization to the middle cortical layers under the condition that pial vein contributions can be removed as these also showed a post-stimulus undershoot.

Jin et al, also in cat visual cortex, showed a post-stimulus undershoot for BOLD, CBF and MION-derived CBV responses, and indicated that the undershoot has a stimulus duration dependence (Jin and Kim, 2008a). When normalized by the peak amplitude, the largest undershoots were found in the middle cortical layers for BOLD, CBF, and CBV. Clear post-stimulus undershoots were observed for long stimulation durations (60s), however almost no post-stimulus undershoot was found for the CBF and CBV responses for shorter stimulation durations (20s). Silva et al came to a similar conclusion in rat somatosensory cortex; for longer stimulus durations (4s, Silva and Koretsky, 2002a) a BOLD undershoot was found whereas in another study using much shorter stimulus durations no undershoot was detected (Silva et al., 2007).

In another study in rat somatosensory cortex, BOLD, CBF and MION-derived CBV responses showed a post-stimulus undershoot for BOLD but not for CBF and CBV for any of the cortical layers, using 20s forepaw stimulation (Shen et al., 2008). This would argue against a hemodynamic origin (sustained elevated CBV and/or a CBF undershoot) of the post-stimulus undershoot. A distinct BOLD post-stimulus undershoot was observed in layers 1–3, which was proposed to be related to the elevated post-stimulus CMRO2 changes in layers 4–6 and may indicate a metabolic origin for the BOLD post-stimulus undershoot (Shen et al., 2008). In what way CMRO2 changes in deeper layers 4–6 would interact with upper layers 1–3, producing a BOLD post-stimulus undershoot only at these locations was not proposed, but would likely rely on passive draining of HbR-rich blood by the upper layers. Hirano et al also reported a small BOLD post-stimulus undershoot in rat somatosensory cortex for different stimulation durations, however its amplitude did not depend on stimulus duration. No CBF or CBV post-stimulus undershoot was detected for any of the stimulus durations or layers (Hirano et al., 2011). The authors did however observe a prolonged elevated CBV response in layers 1–3 and 4–5 that could contribute to the observed BOLD post-stimulus undershoot. Interestingly, Poplawsky et al found distinctly elicited BOLD post-stimulus undershoots in rat olfactory bulb that were more localized to neuronal active layers for most stimulation types (odor and anterior commissure

stimulation) compared to the more poorly localized positive BOLD response (Poplawsky et al., 2015). For the mentioned stimulation types and associated neuronal layers, a sustained elevated CBV response can be observed during the BOLD post-stimulus undershoot. This was, however, not consistent for other stimulation types and layers.

To reconcile the findings on the origin of the post-stimulus undershoot of the BOLD response and its potential application proves to be difficult. This is likely due to the fact that changes in CBV and CBF in different vascular compartments, arterioles, capillary and venules, are dependent on stimulus type and duration, which in turn would also affect the underlying metabolic demand. In addition, the exact role of CBF in the BOLD undershoot remains ambiguous as measurements with high spatiotemporal resolution are challenging due to low sensitivity. Optical imaging studies indicate a reduction in CBF by vasoconstriction in upper cortical layers which can be associated with the post-stimulus undershoot (Chen et al., 2011; Hillman et al., 2007; Srinivasan and Radhakrishnan, 2014). However, the undershoot in middle cortical regions may have different origins, perhaps not resolved with optical imaging. Further, direct measurements of CMRO2 changes using MRI remain unavailable.

Similar to the post-stimulus undershoot, early negative BOLD changes, dubbed the “initial dip”, could be a result of an early change in HbR or HbT and may provide useful insight in neurovascular coupling processes across cortical layers or improve spatial localization to neuronal activity. For practical applications of the initial dip, however, one has to keep in mind that the initial dip signal is of much lower amplitude than the positive and post-stimulus undershoot of a typical BOLD response. Tian et al investigated the initial dip of the BOLD response in rat somatosensory cortex and showed a clear cortical-depth dependency (Tian et al., 2010). Interestingly, the initial dip signal mostly preceded the vessel dilations as measured by two-photon microscopy. The largest initial dip occurred in superficial layers that also showed the slowest vascular response onset times. The occurrence of the largest initial dip in superficial layers can also be observed in the BOLD timecourses in the work of Silva et al, although not explicitly reported (Silva et al., 2007, Figure 5). This finding would be consistent with the notion that the initial dip originates from early oxygen consumption before increases in blood flow and volume changes. Moreover, the findings by Tian et al can explain earlier disagreements between optical imaging and BOLD fMRI. Optical imaging signals are mostly weighted toward the superficial layers, hence more sensitive to the initial dip, whereas the conventionally larger voxel sizes used in BOLD fMRI likely result in reduced sensitivity to initial dip through partial volume effects.

Recent work by Yu et al in rat barrel cortex showed that it is possible to investigate spatiotemporal characteristics of the BOLD response at the level of individual intracortical vessels across cortical depth and compare them to adjacent tissue responses (Yu et al., 2012). The earliest BOLD responses, 0.8s after stimulation, were found in layers 4–5 in the microvasculature of the barrel cortex. Slightly later time points, 1.2s after stimulation, revealed a distinct propagation of the BOLD signal to the macrovasculature, i.e. penetrating intracortical veins and venules, with 2–3 times higher amplitude than that of microvasculature. At even later time points, 1.6s after stimulation, BOLD signal changes were detected relatively far (1–1.5mm) from the activated barrel cortex. This study showed

that later phases of the BOLD response are dominated by penetrating macro-vessels, even in deep cortical layers. In addition to draining veins on cortical surface, penetrating macro-vessels, located 300–500μm apart in rat whisker barrel somatosensory area, can mislocate BOLD responses from the active neuronal sources.

Using a line-scanning method for fMRI, Yu et al obtained very high spatiotemporal (50μm, 50ms) BOLD information (Yu et al., 2014). Within rat barrel, motor and somatosensory cortex, laminar locations of fMRI onset times were found to coincide with distinct neuronal input positions (Figure 3B). Interestingly, using a cortical plasticity model via peripheral denervation, they observed a shift in fMRI onset laminar location that followed the neural input change due to plasticity.

Very recently, Yu et al showed with a similar methodology single vessel BOLD and iron-oxide derived CBV responses in deep cortical layers upon visual and optogenetic stimulation (Yu et al., 2016). With these direct vessel measurements, they found that BOLD responses originate from venules whereas CBV responses originate from feeding arterioles, 0.8s apart. Being able to resolve single vessel BOLD and CBV responses in deep layers using fMRI has benefits compared to two-photon microscopy and other optical imaging methods as it does not require to open the skull (non-invasive), has similar temporal resolution (100ms), and allows investigation of subcortical regions that are elusive to optical methods. Finally, using optogenetics Yu et al demonstrated the potential to investigate individual vessel coupling relationships to specific nearby targeted neuronal circuits.

Human studies

In humans, temporal features of the BOLD response across cortical depth have been thoroughly investigated by Siero et al (Siero et al., 2015; Siero et al., 2011; Siero et al., 2013). Using 7T MRI for increased sensitivity, increased BOLD contrast, and increased microvascular weighting, BOLD activation could be robustly detected across cortical depth with high temporal resolution (between 0.44s and 0.88s) (Figure 3C). Using a fast event-related fMRI design and short stimulation durations (0.25s), detailed characterization of the BOLD response was achieved within an acceptable scan time for human participants (≤10min). Here, short stimulation duration and appropriately chosen inter-stimulus intervals (ISI) (>2.5s) are advised to avoid nonlinearities and large passive blood accumulation in the venous vasculature (Hirano et al., 2011; Miezin et al., 2000; Pfeuffer et al., 2003). The findings by Siero et al are largely in line with findings in animal work. BOLD responses in deep cortical layers are faster in onset time (~1.25s) and TTP, have a narrower FWHM and a smaller amplitude. This spatiotemporal heterogeneity across cortical depth of the BOLD response was found to be in line with the known vascular organization and global blood transit through the vasculature (Duvernoy et al., 1981; Stefanovic et al., 2008; Weber et al., 2008).

In human visual cortex, the initial dip was largest in superficial cortical layers (Siero et al., 2015), consistent with previously reported upstream propagation of vasodilation along the diving arterioles in animals (Tian et al., 2010). This might also explain the difficulty in detecting the BOLD initial dip at lower spatial and temporal resolutions and lower field strengths. Although using the initial dip to map fMRI activation remains very difficult, the

initial dip can give useful insight in laminar-specific neurovascular coupling mechanisms. This was also suggested for negative BOLD responses in general in a study on primates (Goense et al., 2012).

The BOLD post-stimulus undershoot showed different relationships across the cortical depth with respect to stimulus duration, depending on whether normalization by the positive BOLD response was performed. This was performed to partially correct for blood volume and draining effects (Siero et al., 2015). In general, the post-stimulus undershoot is best observable for stimulation durations >1s. The absolute BOLD post-stimulus undershoot was found largest in upper cortical layers, in line with the study by Jin et al in cats(Jin and Kim, 2008a). Interestingly, the normalized post-stimulus undershoot was largest in deeper cortical layers, especially for longer stimulation durations (>2s), in line with high-resolution studies in cats (Yacoub et al., 2006; Zhao et al., 2007). Comparing gradient-echo and spin-echo BOLD using dedicated surface coils (Petridou et al., 2013) demonstrated that microvascular hemodynamics are the main contributor to the early phase of the gradient-echo BOLD response in deep cortical layers (purple curve in Figure 3C), in line with findings in animals (Jin and Kim, 2008a; Silva and Koretsky, 2002; Yu et al., 2012).

In summary, in the human brain differences in BOLD onset time between upper and deep layers (~0.3s) are seemingly faster than the arterial-venous transit time across cortical depth (~1s), suggesting a microvascular origin and thus a locally induced BOLD response (Siero et al., 2011; Siero et al., 2013). This notion opens up the possibility to for study laminar specific neurovascular coupling relationships in the human brain.

Conclusions

Temporal features of the hemodynamic response across cortical depth offer a means to improve the specificity of laminar fMRI to the microvasculature that serves active neuronal sites. The hemodynamic response affords high specificity to the capillary bed perfusing active neurons at early stages of the response (order of 0.5s– 1s), as observed in optical imaging and laminar fMRI studies reviewed here. In laminar fMRI studies, the CBV onset in middle and upper cortical depths is observed first, as predicted by vasodilation in the arterial microvasculature and increased blood volume (Berwick et al., 2005; Chen et al., 2011; Hillman et al., 2007; Srinivasan and Radhakrishnan, 2014; Stefanovic et al., 2008; Tian et al., 2010). This is followed by increases in CBF (Hirano et al., 2011; Shen et al., 2008; Silva et al., 2000 in rat somatosensory cortex) and BOLD (~0.6s to 0.8s, in rat somatosensory cortex, Silva and Koretsky, 2002; Tian et al., 2010; Yu et al., 2012; Yu et al., 2014) in line with upstream (arterial) and downstream (capillary bed and venous network) propagation and increases in blood flow and oxygenation. The onset times of these contrasts can elucidate input neuronal layers in the case of sensory stimulation (thalamo-cortical connections) (Hirano et al., 2011; Siero et al., 2011; Siero et al., 2013; Silva and Koretsky, 2002; Tian et al., 2010; Yu et al., 2014) and of intra-cortical communication (cortico-cortical connections) notably observed using BOLD (Yu et al., 2014). Different studies, however, have used alternate definitions of the onset time; a standard deviation change from baseline, a certain percentage of the positive BOLD response or fitting a slope to a fraction of the rising BOLD response slope (Hirano et al., 2011; Siero et al., 2011; Siero et al., 2013; Silva

and Koretsky, 2002; Tian et al., 2010). Using a standard deviation change from baseline would likely be the ideal approach as it is the least affected by later time points of the BOLD response which may contain non-specific macro-vascular contributions. However, onset times defined as such would depend on the temporal noise level and baseline fluctuations, which should be quantified and reported accordingly. Future work seems warranted to compare the different definitions, preferably under different experimental conditions, such as field strength, MRI sequence, but also for different brain regions and stimulus types and strengths. Differences in onset times of the hemodynamic response across laminae have the potential to resolve laminar neurovascular coupling, and possibly allow the identification of neuronal processes across laminae.

Notably neuronal activity spreads across layers much faster than the onset of hemodynamic responses, on the order of few ms vs. few 100 ms, and it is unclear what mechanism causes this delay between layers. The onset of hemodynamic responses in different layers likely depends on the timing of local neurovascular coupling, for instance the release of vasoactive agents which may in turn depend on the amplitude and nature of the neuronal response across layers. In the case of thalamo-cortical input, faster onset times in upper layers than the transit time of blood through the vasculature suggests the contribution of local neurovascular control. In addition, the onset likely depends on the properties of the local micro-vasculature, for instance the time it takes for vessels to dilate and the mechanism via which this dilation occurs (Tian et al., 2010). The onset of the response in a given layer would likely depend on the balance between these two mechanisms. Interestingly though the findings of Yu and colleagues (Yu et al., 2014) indicate that the onset of the hemodynamic response also depends on neuronal input; for rat barrel cortex, the authors showed that the onset times in layer 4 in the case of thalamo-cortical input and the onset times in layers 2/3 and 5 in the case of cortico-cortical input were of the same order. The authors proposed three possible explanations for their findings: the vasculature in layers receiving input dilates first; early stages of neurovascular coupling that lead to vasodilation may be driven by input activity; neuronal activity in layers receiving input may be more synchronous and lead to a more coordinated vascular response than that in layers that activate via local signal propagation. It may be however that vascular responses in layers that do not receive input directly are fast but not precisely time locked to the stimulus, thus the onset of these responses may be less clear due to averaging of variable responses (Yu et al., 2014, Supplementary Figure 6). Accurate single event measurements would be needed to test this notion. Overall, these findings suggest that local neurovascular coupling and/or properties of the microvasculature may be tuned to respond faster where neuronal input arrives, while the onset of hemodynamics in layers not receiving input directly appear delayed despite the rapid spread of neuronal activity across layers, thus enabling the identification of input activity with fMRI based on onset times. Feedback and feedforward signals arrive in different layers, so it may be possible to identify these signals based on onset times if these are shorter that the transit time of blood through the vasculature. To resolve feedback and feedforward signals across layers, however, will most likely require tailored experiment designs to target the different neuronal processes. Nevertheless, the mechanism that drives the onset of the hemodynamic response across layers is unclear, and poses a challenging

question for further investigations into possible laminar differences in neurovascular coupling and in the properties of the local microvasculature.

In humans, BOLD is a preferred candidate for measuring onset times of the hemodynamic response across cortical depth, because it allows for high sensitivity and spatiotemporal resolution, albeit in confined parts of the brain (Siero et al., 2011; Siero et al., 2013). CBV weighted fMRI measurements, as have been performed in animals, are largely prohibitive in humans when using iron-oxide based contrast agents such as MION. Recently, however, Huber et al compared BOLD and VASO-derived CBV time courses for upper, middle and deep cortical regions in human motor cortex (Huber et al., 2015). Although a high in-plane spatial resolution (<1mm) can be achieved for VASO fMRI, the required inversion time(s) for adequate blood nulling and schemes to correct for BOLD contamination result in a rather poor temporal resolution (~3s), impeding accurate spatiotemporal characterization of VASO-derived CBV responses across cortical depth. Instead of T1-weighted based CBV approaches such as VASO, which have inherently poor temporal resolution, T2* weighted based CBV approaches could be explored. For instance, using non-invasive hyperoxia challenges and fast T2* weighted imaging at high fields strengths ≥7T for high contrast-to-noise (Bulte et al., 2007), or invasive approaches using iron-oxide based agents such as ferumoxytol with no nephrogenic systemic fibrosis risk. Ferumoxytol has recently been FDA approved for human usage as an alternative to gadolinium-based agents (Bashir et al., 2015). The FDA approval, however, is restricted to anemia treatment, and usage as MRI contrast agent is regarded as off-label use of the drug. For more information on ferumoxytol for MRI, see a recent review by Vasanawala et al (Vasanawala et al., 2016). Currently, similar challenges as for VASO exist for ASL based CBF measurements with high spatiotemporal resolution; blood nulling and BOLD contamination correction will result in poor temporal resolution, impeding accurate hemodynamic response characterization.

At later stages of the hemodynamic response, CBV appears to have an advantage in terms of specificity to the microvasculature as compared to BOLD (Hirano et al., 2011; Jin and Kim, 2008a; Silva et al., 2007; Yu et al., 2016). The TTP and FWHM of the BOLD response across cortical depth is longer and wider than that of CBV (Hirano et al., 2011; Silva et al., 2007), and shifted towards the macro-vasculature (Yu et al., 2012) in line with the spread of the hemodynamic response across the venous vasculature. This is also in line with the observation that the FWHM of the point spread function of the BOLD response increases over time (Shmuel et al., 2007). Therefore, BOLD signals originating from local neuronal activity and blood draining though the vasculature combine. Recent advances in models accounting for blood draining and pooling across cortical depth (Heinzle et al., 2016; Markuerkiaga et al., 2016) and for non-separable spatiotemporal dynamics of the hemodynamic response (Aquino et al., 2014) may help to separate vascular from neuronal contributions to the BOLD hemodynamic response across lamina at later stages of the response (see Uludag and Blinder, 2017 for review). Other temporal features of the BOLD response such as the post-stimulus undershoot and initial dip are more debatable both in terms of detectability and exact mechanisms. These negative BOLD signal changes, however, might provide useful insight in laminar neurovascular coupling relationships. Further investigation of these features is warranted to understand what they can tell us.

Despite the potential of temporal features of hemodynamic response, particularly for onset times, to offer additional insights for laminar fMRI investigations, there are several methodological challenges that need to be addressed. The requirements for high spatial and temporal resolution combined are a challenge, translating to losses in signal-to-noise, contrast-to-noise, and reduced brain coverage. High spatial resolution (<1mm) typically comes at the cost of low temporal resolution, which can be balanced, to a certain extent, by reducing the field-of-view of the volume imaged. Signal-to-noise but also contrast-to –noise are often enhanced with the use of surface coils, even at high fields (>7T) (Petridou et al., 2013). Therefore, high spatiotemporal resolution laminar fMRI appears restricted to high field investigations, which limits its application for human studies as the availability of high field scanners is limited as compared to lower field strengths. Further developments in MRI hardware technologies and acquisition methods are likely required to enable the required high spatiotemporal resolution for whole brain coverage. In terms of contrast mechanisms, currently gradient echo BOLD has the highest sensitivity to hemodynamic changes and thus is the most suitable candidate for accurate characterization of hemodynamic responses across the cortical depth. As discussed previously, spin-echo BOLD has higher microvascular specificity but currently lacks adequate sensitivity to resolve detailed BOLD responses across cortical depth. For human applications, current CBV and CBF methods such as VASO and ASL are hampered by low temporal resolution.

In this review we outline temporal features of the hemodynamic response, as measured in optical imaging and laminar fMRI studies. We suggest that these temporal features, particularly the onset of the response, can offer insights on neurovascular coupling, neuronal processing and activity location across laminae.

Acknowledgments

This work has supported by a Netherlands Organization for Scientific Research (NWO) Vidi Grant 13339 (N.P.) and the National Institute of Mental Health of the National Institutes of Health under award number R01MH111417. The Spinoza Centre is a joint initiative of the University of Amsterdam, Academic Medical Center, VU University, VU University Medical Center, Netherlands Institute for Neuroscience and the Royal Netherlands Academy of Sciences.

References

Adams DL, Piserchia V, Economides JR, Horton JC. 2015; Vascular Supply of the Cerebral Cortex is Specialized for Cell Layers but Not Columns. Cereb Cortex. 25:3673–3681. [PubMed: 25246513]

Ahveninen J, Chang WT, Huang S, Keil B, Kopco N, Rossi S, Bonmassar G, Witzel T, Polimeni JR. 2016; Intracortical depth analyses of frequency-sensitive regions of human auditory cortex using 7TfMRI. Neuroimage. 143:116–127. [PubMed: 27608603]

Aquino KM, Robinson PA, Schira MM, Breakspear M. 2014; Deconvolution of neural dynamics from fMRI data using a spatiotemporal hemodynamic response function. Neuroimage. 94:203–215. [PubMed: 24632091]

Barth M, Breuer F, Koopmans PJ, Norris DG, Poser BA. 2016; Simultaneous multislice (SMS) imaging techniques. Magn Reson Med. 75:63–81. [PubMed: 26308571]

Bashir MR, Bhatti L, Marin D, Nelson RC. 2015; Emerging applications for ferumoxytol as a contrast agent in MRI. J Magn Reson Imaging. 41:884–898. [PubMed: 24974785]

Bell MA, Ball MJ. 1985; Laminar variation in the microvascular architecture of normal human visual cortex (area 17). Brain Res. 335:139–143. [PubMed: 4005537]

Berwick J, Johnston D, Jones M, Martindale J, Martin C, Kennerley AJ, Redgrave P, Mayhew JE. 2008; Fine detail of neurovascular coupling revealed by spatiotemporal analysis of the hemodynamic response to single whisker stimulation in rat barrel cortex. J Neurophysiol. 99:787–798. [PubMed: 18046008]

Berwick J, Johnston D, Jones M, Martindale J, Redgrave P, McLoughlin N, Schiessl I, Mayhew JE. 2005; Neurovascular coupling investigated with two-dimensional optical imaging spectroscopy in rat whisker barrel cortex. Eur J Neurosci. 22:1655–1666. [PubMed: 16197506]

Blinder P, Tsai PS, Kaufhold JP, Knutsen PM, Suhl H, Kleinfeld D. 2013; The cortical angiome: an interconnected vascular network with noncolumnar patterns of blood flow. Nat Neurosci. 16:889–897. [PubMed: 23749145]

Brodmann, K. Vergleichende Lokalisationslehre der Großhirnrinde in ihren Prinzipien dargestellt auf Grund des Zellenbaues. Barth, Leipzig: 1909.

Buckner RL, Bandettini PA, O'Craven KM, Savoy RL, Petersen SE, Raichle ME, Rosen BR. 1996; Detection of cortical activation during averaged single trials of a cognitive task using functional magnetic resonance imaging. Proc Natl Acad Sci U S A. 93:14878–14883. [PubMed: 8962149]

Buffalo EA, Fries P, Landman R, Buschman TJ, Desimone R. 2011; Laminar differences in gamma and alpha coherence in the ventral stream. Proc Natl Acad Sci U S A. 108:11262–11267. [PubMed: 21690410]

Bulte D, Chiarelli P, Wise R, Jezzard P. 2007; Measurement of cerebral blood volume in humans using hyperoxic MRI contrast. J Magn Reson Imaging. 26:894–899. [PubMed: 17896390]

Chen BR, Bouchard MB, McCaslin AF, Burgess SA, Hillman EM. 2011; High-speed vascular dynamics of the hemodynamic response. Neuroimage. 54:1021–1030. [PubMed: 20858545]

Chen JJ, Pike GB. 2009; Origins of the BOLD post-stimulus undershoot. Neuroimage. 46:559–568. [PubMed: 19303450]

Chen Y, Aguirre AD, Ruvinskaya L, Devor A, Boas DA, Fujimoto JG. 2009; Optical coherence tomography (OCT) reveals depth-resolved dynamics during functional brain activation. J Neurosci Methods. 178:162–173. [PubMed: 19121336]

Culver JP, Siegel AM, Franceschini MA, Mandeville JB, Boas DA. 2005; Evidence that cerebral blood volume can provide brain activation maps with better spatial resolution than deoxygenated hemoglobin. Neuroimage. 27:947–959. [PubMed: 16084112]

De Martino F, Moerel M, Ugurbil K, Goebel R, Yacoub E, Formisano E. 2015; Frequency preference and attention effects across cortical depths in the human primary auditory cortex. Proc Natl Acad Sci U S A. 112:16036–16041. [PubMed: 26668397]

De Martino F, Zimmermann J, Muckli L, Ugurbil K, Yacoub E, Goebel R. 2013; Cortical depth dependent functional responses in humans at 7T: improved specificity with 3D GRASE. PLoS One. 8:e60514. [PubMed: 23533682]

Devor A, Sakadzic S, Srinivasan VJ, Yaseen MA, Nizar K, Saisan PA, Tian P, Dale AM, Vinogradov SA, Franceschini MA, Boas DA. 2012; Frontiers in optical imaging of cerebral blood flow and metabolism. J Cereb Blood Flow Metab. 32:1259–1276. [PubMed: 22252238]

Devor A, Tian P, Nishimura N, Teng IC, Hillman EM, Narayanan SN, Ulbert I, Boas DA, Kleinfeld D, Dale AM. 2007; Suppressed neuronal activity and concurrent arteriolar vasoconstriction may explain negative blood oxygenation level-dependent signal. J Neurosci. 27:4452–4459. [PubMed: 17442830]

Drew PJ, Shih AY, Kleinfeld D. 2011; Fluctuating and sensory-induced vasodynamics in rodent cortex extend arteriole capacity. Proc Natl Acad Sci U S A. 108:8473–8478. [PubMed: 21536897]

Dumoulin SO, Fracasso A, van der Zwaag W, Siero JC, Petridou N. 2017Ultra-high field MRI: Advancing systems neuroscience towards mesoscopic human brain function. Neuroimage.

Dunn AK, Devor A, Dale AM, Boas DA. 2005; Spatial extent of oxygen metabolism and hemodynamic changes during functional activation of the rat somatosensory cortex. Neuroimage. 27:279–290. [PubMed: 15925522]

Duvernoy HM, Delon S, Vannson JL. 1981; Cortical blood vessels of the human brain. Brain Res Bull. 7:519–579. [PubMed: 7317796]

Feinberg DA, Yacoub E. 2012; The rapid development of high speed, resolution and precision in fMRI. Neuroimage. 62:720–725. [PubMed: 22281677]

Felleman DJ, Van Essen DC. 1991; Distributed hierarchical processing in the primate cerebral cortex. Cereb Cortex. 1:1–47. [PubMed: 1822724]

Fracasso A, Luijten PR, Dumoulin SO, Petridou N. 2017Laminar imaging of positive and negative BOLD in human visual cortex at 7T. Neuroimage.

Fracasso A, Petridou N, Dumoulin SO. 2016; Systematic variation of population receptive field properties across cortical depth in human visual cortex. Neuroimage. 139:427–438. [PubMed: 27374728]

Friston KJ, Josephs O, Rees G, Turner R. 1998; Nonlinear event-related responses in fMRI. Magn Reson Med. 39:41–52. [PubMed: 9438436]

Gardumi A, Ivanov D, Havlicek M, Formisano E, Uludag K. 2017; Tonotopic maps in human auditory cortex using arterial spin labeling. Hum Brain Mapp. 38:1140–1154. [PubMed: 27790786]

Givre SJ, Schroeder CE, Arezzo JC. 1994; Contribution of extrastriate area V4 to the surfacerecorded flash VEP in the awake macaque. Vision Res. 34:415–428. [PubMed: 8303826]

Goense J, Merkle H, Logothetis NK. 2012; High-resolution fMRI reveals laminar differences in neurovascular coupling between positive and negative BOLD responses. Neuron. 76:629–639. [PubMed: 23141073]

Goense JB, Logothetis NK. 2006; Laminar specificity in monkey V1 using high-resolution SE-fMRI. Magn Reson Imaging. 24:381–392. [PubMed: 16677944]

Goense JB, Zappe AC, Logothetis NK. 2007; High-resolution fMRI of macaque V1. Magn Reson Imaging. 25:740–747. [PubMed: 17499466]

Graham J, Lin CS, Kaas JH. 1979; Subcortical projections of six visual cortical areas in the owl monkey, Aotus trivirgatus. J Comp Neurol. 187:557–580. [PubMed: 114555]

Grinvald A, Slovin H, Vanzetta I. 2000; Non-invasive visualization of cortical columns by fMRI. Nat Neurosci. 3:105–107. [PubMed: 10649563]

Guidi M, Huber L, Lampe L, Gauthier CJ, Moller HE. 2016; Lamina-dependent calibrated BOLD response in human primary motor cortex. Neuroimage. 141:250–261. [PubMed: 27364473]

Haegens S, Barczak A, Musacchia G, Lipton ML, Mehta AD, Lakatos P, Schroeder CE. 2015; Laminar Profile and Physiology of the alpha Rhythm in Primary Visual, Auditory, and Somatosensory Regions of Neocortex. J Neurosci. 35:14341–14352. [PubMed: 26490871]

Hall CN, Reynell C, Gesslein B, Hamilton NB, Mishra A, Sutherland BA, O'Farrell FM, Buchan AM, Lauritzen M, Attwell D. 2014; Capillary pericytes regulate cerebral blood flow in health and disease. Nature. 508:55–60. [PubMed: 24670647]

Harel N, Lin J, Moeller S, Ugurbil K, Yacoub E. 2006; Combined imaging-histological study of cortical laminar specificity of fMRI signals. Neuroimage. 29:879–887. [PubMed: 16194614]

Harrison RV, Harel N, Panesar J, Mount RJ. 2002; Blood capillary distribution correlates with hemodynamic-based functional imaging in cerebral cortex. Cereb Cortex. 12:225–233. [PubMed: 11839597]

Heinzle J, Koopmans PJ, den Ouden HE, Raman S, Stephan KE. 2016; A hemodynamic model for layered BOLD signals. Neuroimage. 125:556–570. [PubMed: 26484827]

Herman P, Sanganahalli BG, Blumenfeld H, Rothman DL, Hyder F. 2013; Quantitative basis for neuroimaging of cortical laminae with calibrated functional MRI. Proc Natl Acad Sci U S A. 110:15115–15120. [PubMed: 23980158]

Hill RA, Tong L, Yuan P, Murikinati S, Gupta S, Grutzendler J. 2015; Regional Blood Flow in the Normal and Ischemic Brain Is Controlled by Arteriolar Smooth Muscle Cell Contractility and Not by Capillary Pericytes. Neuron. 87:95–110. [PubMed: 26119027]

Hillman EM. 2014; Coupling mechanism and significance of the BOLD signal: a status report. Annu Rev Neurosci. 37:161–181. [PubMed: 25032494]

Hillman EM, Devor A, Bouchard MB, Dunn AK, Krauss GW, Skoch J, Bacskai BJ, Dale AM, Boas DA. 2007; Depth-resolved optical imaging and microscopy of vascular compartment dynamics during somatosensory stimulation. Neuroimage. 35:89–104. [PubMed: 17222567]

Hirano Y, Stefanovic B, Silva AC. 2011; Spatiotemporal evolution of the functional magnetic resonance imaging response to ultrashort stimuli. J Neurosci. 31:1440–1447. [PubMed: 21273428]

Hubel DH, Wiesel TN. 1972; Laminar and columnar distribution of geniculo-cortical fibers in the macaque monkey. J Comp Neurol. 146:421–450. [PubMed: 4117368]

Huber L, Goense J, Kennerley AJ, Ivanov D, Krieger SN, Lepsien J, Trampel R, Turner R, Moller HE. 2014; Investigation of the neurovascular coupling in positive and negative BOLD responses in human brain at 7 T. Neuroimage. 97:349–362. [PubMed: 24742920]

Huber L, Goense J, Kennerley AJ, Trampel R, Guidi M, Reimer E, Ivanov D, Neef N, Gauthier CJ, Turner R, Moller HE. 2015; Cortical lamina-dependent blood volume changes in human brain at 7 T. Neuroimage. 107:23–33. [PubMed: 25479018]

Iadecola C, Yang G, Ebner TJ, Chen G. 1997; Local and propagated vascular responses evoked by focal synaptic activity in cerebellar cortex. J Neurophysiol. 78:651–659. [PubMed: 9307102]

Jin T, Kim SG. 2008a; Cortical layer-dependent dynamic blood oxygenation, cerebral blood flow and cerebral blood volume responses during visual stimulation. Neuroimage. 43:1–9. [PubMed: 18655837]

Jin T, Kim SG. 2008b; Improved cortical-layer specificity of vascular space occupancy fMRI with slab inversion relative to spin-echo BOLD at 9.4 T. Neuroimage. 40:59–67. [PubMed: 18249010]

Kemper VG, De Martino F, Vu AT, Poser BA, Feinberg DA, Goebel R, Yacoub E. 2015; Sub-millimeter T2 weighted fMRI at 7 T: comparison of 3D-GRASE and 2D SE-EPI. Front Neurosci. 9:163. [PubMed: 25999810]

Kim SG, Ogawa S. 2012; Biophysical and physiological origins of blood oxygenation level-dependent fMRI signals. J Cereb Blood Flow Metab. 32:1188–1206. [PubMed: 22395207]

Kim T, Hendrich KS, Masamoto K, Kim SG. 2007; Arterial versus total blood volume changes during neural activity-induced cerebral blood flow change: implication for BOLD fMRI. J Cereb Blood Flow Metab. 27:1235–1247. [PubMed: 17180136]

Kim T, Kim SG. 2010; Cortical layer-dependent arterial blood volume changes: improved spatial specificity relative to BOLD fMRI. Neuroimage. 49:1340–1349. [PubMed: 19800013]

Kim T, Kim SG. 2011; Temporal dynamics and spatial specificity of arterial and venous blood volume changes during visual stimulation: implication for BOLD quantification. J Cereb Blood Flow Metab. 31:1211–1222. [PubMed: 21179068]

Kok P, Bains LJ, van Mourik T, Norris DG, de Lange FP. 2016; Selective Activation of the Deep Layers of the Human Primary Visual Cortex by Top-Down Feedback. Curr Biol. 26:371–376. [PubMed: 26832438]

Koopmans PJ, Barth M, Norris DG. 2010; Layer-specific BOLD activation in human V1. Hum Brain Mapp. 31:1297–1304. [PubMed: 20082333]

Koopmans PJ, Barth M, Orzada S, Norris DG. 2011; Multi-echo fMRI of the cortical laminae in humans at 7 T. Neuroimage. 56:1276–1285. [PubMed: 21338697]

Lee AT, Glover GH, Meyer CH. 1995; Discrimination of large venous vessels in time-course spiral blood-oxygen-level-dependent magnetic-resonance functional neuroimaging. Magn Reson Med. 33:745–754. [PubMed: 7651109]

Maier A, Adams GK, Aura C, Leopold DA. 2010Distinct superficial and deep laminar domains of activity in the visual cortex during rest and stimulation. Front Syst Neurosci. :4.

Maier A, Aura CJ, Leopold DA. 2011; Infragranular sources of sustained local field potential responses in macaque primary visual cortex. J Neurosci. 31:1971–1980. [PubMed: 21307235]

Malonek D, Dirnagl U, Lindauer U, Yamada K, Kanno I, Grinvald A. 1997; Vascular imprints of neuronal activity: relationships between the dynamics of cortical blood flow, oxygenation, and volume changes following sensory stimulation. Proc Natl Acad Sci U S A. 94:14826–14831. [PubMed: 9405698]

Malonek D, Grinvald A. 1996; Interactions between electrical activity and cortical microcirculation revealed by imaging spectroscopy: implications for functional brain mapping. Science. 272:551–554. [PubMed: 8614805]

Markuerkiaga I, Barth M, Norris DG. 2016; A cortical vascular model for examining the specificity of the laminar BOLD signal. Neuroimage. 132:491–498. [PubMed: 26952195]

Masamoto K, Kurachi T, Takizawa N, Kobayashi H, Tanishita K. 2004; Successive depth variations in microvascular distribution of rat somatosensory cortex. Brain Res. 995:66–75. [PubMed: 14644472]

Menon RS, Goodyear BG. 1999; Submillimeter functional localization in human striate cortex using BOLD contrast at 4 Tesla: implications for the vascular point-spread function. Magn Reson Med. 41:230–235. [PubMed: 10080267]

Merkle CW, Srinivasan VJ. 2016; Laminar microvascular transit time distribution in the mouse somatosensory cortex revealed by Dynamic Contrast Optical Coherence Tomography. Neuroimage. 125:350–362. [PubMed: 26477654]

Miezin FM, Maccotta L, Ollinger JM, Petersen SE, Buckner RL. 2000; Characterizing the hemodynamic response: effects of presentation rate, sampling procedure, and the possibility of ordering brain activity based on relative timing. Neuroimage. 11:735–759. [PubMed: 10860799]

Mitzdorf U, Singer W. 1979; Excitatory synaptic ensemble properties in the visual cortex of the macaque monkey: a current source density analysis of electrically evoked potentials. J Comp Neurol. 187:71–83. [PubMed: 114553]

Olman CA, Harel N, Feinberg DA, He S, Zhang P, Ugurbil K, Yacoub E. 2012; Layer-specific fMRI reflects different neuronal computations at different depths in human V1. PLoS One. 7:e32536. [PubMed: 22448223]

Petridou N, Italiaander M, van de Bank BL, Siero JC, Luijten PR, Klomp DW. 2013; Pushing the limits of high-resolution functional MRI using a simple high-density multi-element coil design. NMR Biomed. 26:65–73. [PubMed: 22674638]

Pfeuffer J, McCullough JC, Van de Moortele PF, Ugurbil K, Hu X. 2003; Spatial dependence of the nonlinear BOLD response at short stimulus duration. Neuroimage. 18:990–1000. [PubMed: 12725773]

Polimeni JR, Fischl B, Greve DN, Wald LL. 2010; Laminar analysis of 7T BOLD using an imposed spatial activation pattern in human V1. Neuroimage. 52:1334–1346. [PubMed: 20460157]

Poplawsky AJ, Fukuda M, Murphy M, Kim SG. 2015; Layer-Specific fMRI Responses to Excitatory and Inhibitory Neuronal Activities in the Olfactory Bulb. J Neurosci. 35:15263–15275. [PubMed: 26586815]

Reina-De La Torre F, Rodriguez-Baeza A, Sahuquillo-Barris J. 1998; Morphological characteristics and distribution pattern of the arterial vessels in human cerebral cortex: a scanning electron microscope study. Anat Rec. 251:87–96. [PubMed: 9605225]

Ress D, Glover GH, Liu J, Wandell B. 2007; Laminar profiles of functional activity in the human brain. Neuroimage. 34:74–84. [PubMed: 17011213]

Rockland KS, Pandya DN. 1979; Laminar origins and terminations of cortical connections of the occipital lobe in the rhesus monkey. Brain Res. 179:3–20. [PubMed: 116716]

Scheeringa R, Koopmans PJ, van Mourik T, Jensen O, Norris DG. 2016; The relationship between oscillatory EEG activity and the laminar-specific BOLD signal. Proc Natl Acad Sci U S A. 113:6761–6766. [PubMed: 27247416]

Schroeder CE, Mehta AD, Givre SJ. 1998; A spatiotemporal profile of visual system activation revealed by current source density analysis in the awake macaque. Cereb Cortex. 8:575–592. [PubMed: 9823479]

Schroeder CE, Tenke CE, Givre SJ, Arezzo JC, Vaughan HG Jr. 1991; Striate cortical contribution to the surface-recorded pattern-reversal VEP in the alert monkey. Vision Res. 31:1143–1157. [PubMed: 1891808]

Self MW, van Kerkoerle T, Super H, Roelfsema PR. 2013; Distinct roles of the cortical layers of area V1 in figure-ground segregation. Curr Biol. 23:2121–2129. [PubMed: 24139742]

Shen Q, Ren H, Duong TQ. 2008; CBF, BOLD, CBV, and CMRO(2) fMRI signal temporal dynamics at 500-msec resolution. J Magn Reson Imaging. 27:599–606. [PubMed: 18219630]

Shih YY, Chen YY, Lai HY, Kao YC, Shyu BC, Duong TQ. 2013; Ultra high-resolution fMRI and electrophysiology of the rat primary somatosensory cortex. Neuroimage. 73:113–120. [PubMed: 23384528]

Shmuel A, Yacoub E, Chaimow D, Logothetis NK, Ugurbil K. 2007; Spatio-temporal point-spread function of fMRI signal in human gray matter at 7 Tesla. Neuroimage. 35:539–552. [PubMed: 17306989]

Siero JC, Hendrikse J, Hoogduin H, Petridou N, Luijten P, Donahue MJ. 2015; Cortical depth dependence of the BOLD initial dip and poststimulus undershoot in human visual cortex at 7 Tesla. Magn Reson Med. 73:2283–2295. [PubMed: 24989338]

Siero JC, Petridou N, Hoogduin H, Luijten PR, Ramsey NF. 2011; Cortical depth-dependent temporal dynamics of the BOLD response in the human brain. J Cereb Blood Flow Metab. 31:1999–2008. [PubMed: 21505479]

Siero JC, Ramsey NF, Hoogduin H, Klomp DW, Luijten PR, Petridou N. 2013; BOLD specificity and dynamics evaluated in humans at 7 T: comparing gradient-echo and spin-echo hemodynamic responses. PLoS One. 8:e54560. [PubMed: 23336008]

Silva AC, Koretsky AP. 2002; Laminar specificity of functional MRI onset times during somatosensory stimulation in rat. Proc Natl Acad Sci U S A. 99:15182–15187. [PubMed: 12407177]

Silva AC, Koretsky AP, Duyn JH. 2007; Functional MRI impulse response for BOLD and CBV contrast in rat somatosensory cortex. Magn Reson Med. 57:1110–1118. [PubMed: 17534912]

Silva AC, Lee SP, Iadecola C, Kim SG. 2000; Early temporal characteristics of cerebral blood flow and deoxyhemoglobin changes during somatosensory stimulation. J Cereb Blood Flow Metab. 20:201–206. [PubMed: 10616809]

Sirotin YB, Hillman EM, Bordier C, Das A. 2009; Spatiotemporal precision and hemodynamic mechanism of optical point spreads in alert primates. Proc Natl Acad Sci U S A. 106:18390–18395. [PubMed: 19828443]

Spaak E, Bonnefond M, Maier A, Leopold DA, Jensen O. 2012; Layer-specific entrainment of gamma-band neural activity by the alpha rhythm in monkey visual cortex. Curr Biol. 22:2313–2318. [PubMed: 23159599]

Srinivasan VJ, Radhakrishnan H. 2014; Optical Coherence Tomography angiography reveals laminar microvascular hemodynamics in the rat somatosensory cortex during activation. Neuroimage. 102(Pt 2):393–406. [PubMed: 25111471]

Stefanovic B, Hutchinson E, Yakovleva V, Schram V, Russell JT, Belluscio L, Koretsky AP, Silva AC. 2008; Functional reactivity of cerebral capillaries. J Cereb Blood Flow Metab. 28:961–972. [PubMed: 18059431]

Tian P, Teng IC, May LD, Kurz R, Lu K, Scadeng M, Hillman EM, De Crespigny AJ, D'Arceuil HE, Mandeville JB, Marota JJ, Rosen BR, Liu TT, Boas DA, Buxton RB, Dale AM, Devor A. 2010; Cortical depth-specific microvascular dilation underlies laminar differences in blood oxygenation level-dependent functional MRI signal. Proc Natl Acad Sci U S A. 107:15246–15251. [PubMed: 20696904]

Tigges J, Tigges M, Perachio AA. 1977; Complementary laminar terminations of afferents to area 17 originating in area 18 and in the lateral geniculate nucleus in squirrel monkey. J Comp Neurol. 176:87–100. [PubMed: 409740]

Tsai PS, Kaufhold JP, Blinder P, Friedman B, Drew PJ, Karten HJ, Lyden PD, Kleinfeld D. 2009; Correlations of neuronal and microvascular densities in murine cortex revealed by direct counting and colocalization of nuclei and vessels. J Neurosci. 29:14553–14570. [PubMed: 19923289]

Ugurbil K, Xu J, Auerbach EJ, Moeller S, Vu AT, Duarte-Carvajalino JM, Lenglet C, Wu X, Schmitter S, Van de Moortele PF, Strupp J, Sapiro G, De Martino F, Wang D, Harel N, Garwood M, Chen L, Feinberg DA, Smith SM, Miller KL, Sotiropoulos SN, Jbabdi S, Andersson JL, Behrens TE, Glasser MF, Van Essen DC, Yacoub E. 2013; Pushing spatial and temporal resolution for functional and diffusion MRI in the Human Connectome Project. Neuroimage. 80:80–104. [PubMed: 23702417]

Uludag K, Blinder P. 2017Linking brain vascular physiology to hemodynamic response in ultra-high field MRI. Neuroimage.

Uludag K, Muller-Bierl B, Ugurbil K. 2009; An integrative model for neuronal activity-induced signal changes for gradient and spin echo functional imaging. Neuroimage. 48:150–165. [PubMed: 19481163]

Vanzetta I, Hildesheim R, Grinvald A. 2005; Compartment-resolved imaging of activity-dependent dynamics of cortical blood volume and oximetry. J Neurosci. 25:2233–2244. [PubMed: 15745949]

Vasanawala SS, Nguyen KL, Hope MD, Bridges MD, Hope TA, Reeder SB, Bashir MR. 2016; Safety and technique of ferumoxytol administration for MRI. Magn Reson Med. 75:2107–2111. [PubMed: 26890830]

Vazquez AL, Fukuda M, Tasker ML, Masamoto K, Kim SG. 2010; Changes in cerebral arterial, tissue and venous oxygenation with evoked neural stimulation: implications for hemoglobin-based functional neuroimaging. J Cereb Blood Flow Metab. 30:428–439. [PubMed: 19844241]

Weber B, Keller AL, Reichold J, Logothetis NK. 2008; The microvascular system of the striate and extrastriate visual cortex of the macaque. Cereb Cortex. 18:2318–2330. [PubMed: 18222935]

Wiggins GC, Polimeni JR, Potthast A, Schmitt M, Alagappan V, Wald LL. 2009; 96-Channel receive-only head coil for 3 Tesla: design optimization and evaluation. Magn Reson Med. 62:754–762. [PubMed: 19623621]

Wiggins GC, Triantafyllou C, Potthast A, Reykowski A, Nittka M, Wald LL. 2006; 32-channel 3 Tesla receive-only phased-array head coil with soccer-ball element geometry. Magn Reson Med. 56:216–223. [PubMed: 16767762]

Xing D, Yeh CI, Burns S, Shapley RM. 2012; Laminar analysis of visually evoked activity in the primary visual cortex. Proc Natl Acad Sci U S A. 109:13871–13876. [PubMed: 22872866]

Yacoub E, Ugurbil K, Harel N. 2006; The spatial dependence of the poststimulus undershoot as revealed by high-resolution BOLD- and CBV-weighted fMRI. J Cereb Blood Flow Metab. 26:634–644. [PubMed: 16222242]

Yu X, Glen D, Wang S, Dodd S, Hirano Y, Saad Z, Reynolds R, Silva AC, Koretsky AP. 2012; Direct imaging of macrovascular and microvascular contributions to BOLD fMRI in layers IV-V of the rat whisker-barrel cortex. Neuroimage. 59:1451–1460. [PubMed: 21851857]

Yu X, He Y, Wang M, Merkle H, Dodd SJ, Silva AC, Koretsky AP. 2016; Sensory and optogenetically driven single-vessel fMRI. Nat Methods. 13:337–340. [PubMed: 26855362]

Yu X, Qian C, Chen DY, Dodd SJ, Koretsky AP. 2014; Deciphering laminar-specific neural inputs with line-scanning fMRI. Nat Methods. 11:55–58. [PubMed: 24240320]

Zhao F, Jin T, Wang P, Kim SG. 2007; Improved spatial localization of post-stimulus BOLD undershoot relative to positive BOLD. Neuroimage. 34:1084–1092. [PubMed: 17161623]

Zhao F, Wang P, Hendrich K, Ugurbil K, Kim SG. 2006; Cortical layer-dependent BOLD and CBV responses measured by spin-echo and gradient-echo fMRI: insights into hemodynamic regulation. Neuroimage. 30:1149–1160. [PubMed: 16414284]

Zhao F, Wang P, Kim SG. 2004; Cortical depth-dependent gradient-echo and spin-echo BOLD fMRI at 9.4T. Magn Reson Med. 51:518–524. [PubMed: 15004793]

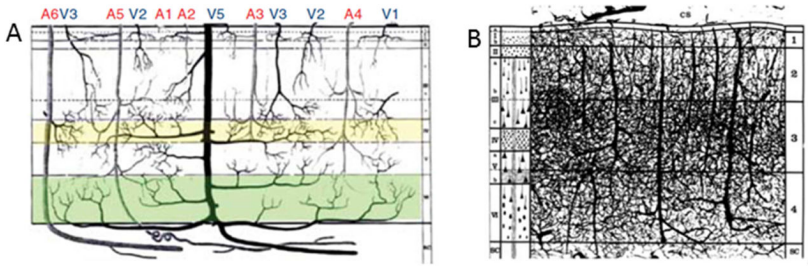

Figure 1.

A) Illustration of the intra-cortical vascular organization according to penetration depth and diameter, from the pial surface (top) to white matter (bottom). *A* denotes arteries and *V* denotes veins, the numbers indicate the vessel group. Group 6 arteries extends to white matter without perfusing the cortex (reproduced from Kim and Ogawa, 2012, adapted from Duvernoy et al., 1981). **B)** Illustration of the intra-cortical vascular according to vascular density. Vascular layers are denoted on the right, neuronal layers are denoted on the left of the schematic (reproduced from Duvernoy et al., 1981)

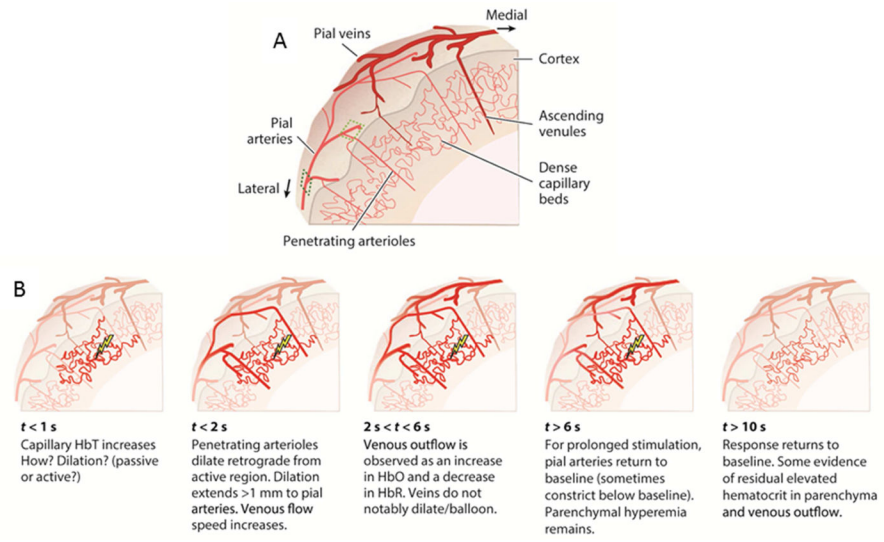

Figure 2.

A) Schematic of cortical vascular tree, illustrating pial veins and arteries, penetrating intracortical arteries that branch into capillary beds, and ascending intracortical veins. **B)** Schematic of the evolution of the hemodynamic response across the vascular tree discussed in the text (adapted from Hillman, 2014)

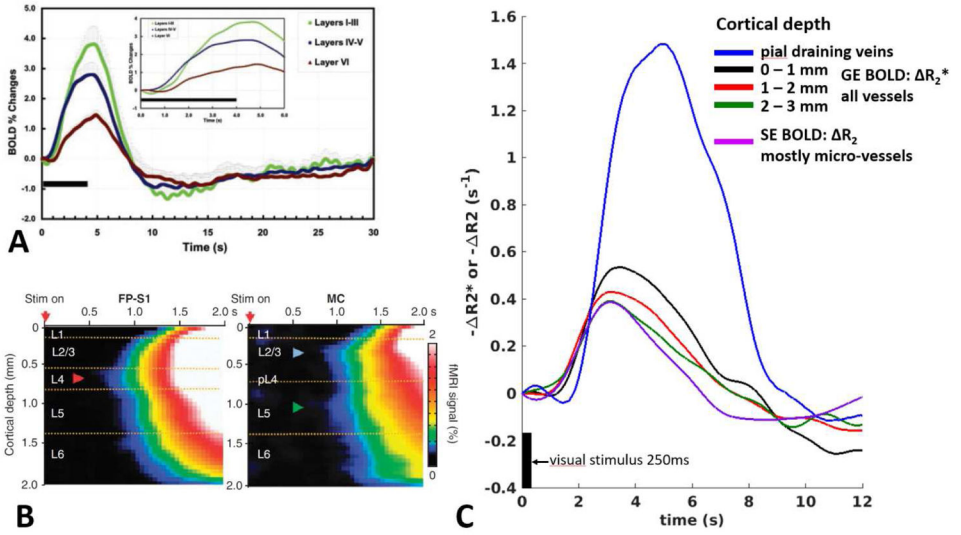

Figure 3.

A) BOLD time courses across cortical laminae in rat somatosensory cortex, acquired with high in-plane spatial and temporal resolution of 200μm and 40ms respectively. One can clearly observe that the BOLD response in layers 4–5 (blue line) is earliest compared to layers 1–3 and 6 (green and red line respectively). Figure adapted from Silva et al PNAS 2002. **B)** Detailed BOLD time course maps across cortical depth using a line-scanning MRI method offering very high spatiotemporal resolution of 50μm and 50ms respectively. Arrowheads point to the earliest fMRI onsets in rat forepaw somatosensory cortex (FP-S1) (red) and in motor cortex (MC) (blue and green). Clearly seen is the early BOLD onset in layer 4 in FP-S1, which coincides with known thalamo-cortical neuronal input activated by forepaw stimulation. In motor cortex, early BOLD onsets are observed in layer 2–3 and 5, which coincide with known somatomotor neuronal connections activated by whisker stimulation. Figure adapted from Yu et al Nature Methods 2014. **C)** Spatiotemporal characteristics of the BOLD response for different vascular contributions in human visual cortex across cortical depth. ΔR2* denotes gradient-echo BOLD signal changes, ΔR2 spin-echo BOLD signal changes at 7T using custom surface coils (TR: 0.88ms) (Petridou et al., 2013). Figure adapted from Siero et al PLOS ONE 2013. Deeper GE BOLD responses (1–2, and 2–3mm cortical depth, red and green lines) are earliest to respond and coincide with the SE BOLD response (purple line), which is mostly weighted by the microvasculature (Uludag et al., 2009).